

Ciliary Targeting of Olfactory CNG Channels Requires the CNGB1b Subunit and the Kinesin-2 Motor Protein, KIF17

Paul M. Jenkins,¹ Toby W. Hurd,³ Lian Zhang,¹ Dyke P. McEwen,¹ R. Lane Brown,⁴ Ben Margolis,^{2,3} Kristen J. Verhey,⁵ and Jeffrey R. Martens^{1,*}

¹Department of Pharmacology
University of Michigan

Ann Arbor, Michigan 48109

²Department of Biological Chemistry
University of Michigan

Ann Arbor, Michigan 48109

³Department of Internal Medicine
University of Michigan

Ann Arbor, Michigan 48109

⁴Neurological Sciences Institute
Oregon Health & Science University
Beaverton, Oregon 97006

⁵Cell and Developmental Biology
University of Michigan
Ann Arbor, Michigan 48109

Summary

Nonmotile cilia on olfactory sensory neurons (OSNs) compartmentalize signaling molecules, including odorant receptors and cyclic nucleotide-gated (CNG) channels, allowing for efficient, spatially confined responses to sensory stimuli [1–3]. Little is known about the mechanisms of the ciliary targeting of olfactory CNG channels, composed of three subunits: CNGA2, CNGA4, and CNGB1b [4]. Recent reports suggest that subunit composition of the retinal CNG channel influences localization, leading to disease [5, 6]. However, the mechanistic role of subunits in properly targeting native olfactory CNG channels remains unclear. Here, we show that heteromeric assembly with CNGB1b, containing a critical carboxy-terminal motif (RVxP), is required for ciliary trafficking of olfactory CNG channels. Movement of proteins within the cilia is governed by intraflagellar transport (IFT), a process that facilitates bidirectional movement of cargo along microtubules [7, 8]. Work in *C. elegans* has established that heterotrimeric and homodimeric kinesin-2 family members play a critical role in anterograde transport [9–11]. In mammalian systems, the heterotrimeric KIF3a/KIF3b/KAP-3 complex plays a clear role in IFT; however, no role has been established for KIF17, the mammalian homolog of OSM-3 [12]. Here, we demonstrate that KIF17 is required for olfactory CNG channel targeting, providing novel insights into mechanisms of mammalian ciliary transport.

Results

To investigate the role of subunit composition in ciliary targeting of olfactory CNG channels, we expressed

yellow fluorescent protein (YFP)-tagged CNGA2 in Madin-Darby canine kidney (MDCK) cells. These cells contain a nonmotile primary cilium extending from their apical surface and are an established heterologous system for the study of mammalian ciliary transport. When expressed alone, CNGA2-YFP was restricted to the cytoplasm and failed to colocalize with acetylated tubulin (0/30 cells), which labels stabilized microtubules including the ciliary axoneme (Figure 1, top). Coexpression of CNGA2-YFP with CNGA4 did not result in any detectable ciliary localization (0/20 cells) (Figure 1, middle) but rather colocalization of the proteins in the cytoplasm (Figure S1). Surprisingly, coexpression of CNGA2-YFP with CNGB1b resulted in the targeting of channel protein to primary cilia where the YFP signal colocalized with both acetylated tubulin (30/30 cells) (Figure 1, bottom) and CNGB1b-3×Flag (Figure S1) in a punctate pattern along the entire length of the cilia (Figure S2). When expressed alone, both CNGA4 and CNGB1b were confined to the cytoplasm, consistent with reports that these subunits do not efficiently form tetramers capable of cell-surface expression [13] (Figure S1).

Amino acid sequence comparison revealed a potential ciliary targeting motif (RVSP; amino acids 821–824) in the carboxy-terminus of CNGB1b (Figure 2A). The RVxP motif has been implicated in the ciliary localization of another membrane protein, polycystin-2 [14], and is absent from both the CNGA2 and CNGA4 subunits (Figure 2A). Mutation of positions R821, V822, and P824 to alanines (AASA mutant) resulted in the loss of ciliary targeting of CNGA2-YFP (Figures 2B and 2C), although this mutant CNGB1b subunit was still able to assemble with CNGA2 as determined by coimmunoprecipitation (Figure S3). In contrast, alanine substitution at position S823 had no effect on CNGA2 localization to cilia, suggesting a specific requirement for the RVxP motif (Figure 2D). Indeed, single alanine substitutions of positions R821, V822, or P824 led to a statistically significant decrease in ciliary targeting (Figure S4). These data are consistent with previous reports describing alanine substitutions of a putative flagellar targeting motif [15]. Notably, insertion of the RVSP motif 26 amino acids from the C terminus of CNGA2 was not sufficient to confer targeting of CNGA2 to the primary cilia (Figure 2E). Together, these data show that heteromeric assembly with CNGB1b is necessary but not sufficient for targeting of olfactory CNG channels to cilia.

Having defined the subunit requirements for olfactory CNG channel targeting to cilia, we next sought to identify the motors responsible for transporting this cargo. Consistent with microtubule-based transport, destabilization of microtubule organization by demecolcine treatment resulted in a loss of cilia and accumulation of CNG channels at the basal body in MDCK cells (Figure S5). To test whether the main IFT anterograde motor kinesin-II plays a role in targeting of CNG channels,

*Correspondence: martensj@umich.edu

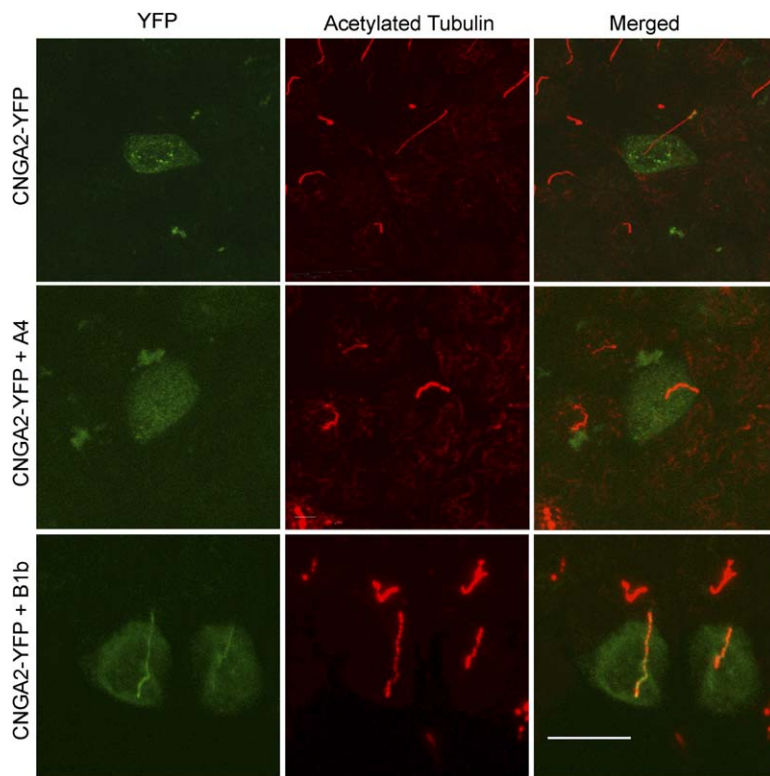


Figure 1. Ciliary Enrichment of CNGA2 Requires CNGB1b but Not CNGA4

Representative images of MDCK cells transfected with CNGA2-YFP alone (top), CNGA2-YFP + CNGA4-3×Flag (middle), or CNGA2-YFP + CNGB1b-3×Flag (bottom). YFP fluorescence is shown at left (green), and immunostaining for acetylated tubulin is shown at center (red). Merged (right) signals from YFP and acetylated tubulin; yellow indicates colocalization. Bar represents 10 μ m.

we transfected MDCK cells with a dominant-negative kinesin-II construct (KIF3aDN) that lacks the motor domain [16]. As predicted, expression of KIF3aDN resulted in a complete loss of cilia, consistent with its role in ciliary assembly and maintenance (Figure S5) [17, 18]. Another kinesin family member, KIFC3, has been implicated in transport of cargo to the minus end of the microtubules at the apical surface of MDCK cells [19]. Interestingly, expression of a dominant-negative KIFC3 construct did not affect targeting of CNG channels to the cilia (Figure S5). Together, these results demonstrate that although the primary machinery for anterograde IFT previously characterized in invertebrates also participates in mammalian ciliary transport, the trafficking of CNG channels to cilia may occur through a novel mechanism.

A second kinesin-2 enzyme, the homodimeric OSM-3 kinesin, has been shown to transport IFT cargoes together with the heterotrimeric kinesin-2 (KLP20/KLP11/KAP-1) complex in *C. elegans* [8]. A role for the mammalian homolog of OSM-3, KIF17, in IFT has not been determined. Rather, KIF17 was proposed to have a brain-specific function in dendritic transport [12]. We show that KIF17 is endogenously expressed in MDCK cell cilia (Figure 3A) as well as in the ciliary layer of the olfactory epithelium (Figure 3B), with a staining pattern indistinguishable from the ciliary-enriched type-III adenylyl cyclase (AC-III) [20] (Figure S6). Furthermore, KIF17 was coimmunoprecipitated with CNGA2 antibodies, demonstrating that endogenous CNG channels and KIF17 are part of a complex in native rat olfactory epithelium (Figures 3F and 3G). To test whether KIF17 plays a role in ciliary transport of CNG channels, MDCK cells were transfected with a dominant-negative KIF17 construct

(KIF17DN). Expression of KIF17DN inhibited ciliary transport of CNG channels (CNGA2-YFP + CNGB1b) as no YFP fluorescence signal was detected in the cilia (Figure 3C) in any of the cells examined (0/11) (Figure 3D). Mislocalization was specific for ciliary proteins as localization of apical and basolateral proteins were unaffected (Figure S7). In addition, expression of full-length KIF17 did not alter CNG channel targeting to cilia (data not shown). Interestingly, unlike KIF3aDN, expression of KIF17DN did not change the average length of primary cilia ($p = 0.7564$, one-way ANOVA), indicating that these two motors may be functionally specialized in mammalian cilia (Figure 3E).

A major technical obstacle to the real-time study of protein movement in living cilia has been the successful expression of fluorescently-tagged proteins in vertebrate cilia. The ciliary targeting of the YFP-CNGA2/CNGB1b complex provided a model to monitor movement of membrane proteins in MDCK cell primary cilia and permitted the first measurements of CNG channel mobility. We used fluorescence recovery after photobleaching (FRAP) to measure CNG channel dynamics in the ciliary compartment. For these experiments, CNGA2 channels were tagged with citrine, a photostable variant of YFP [21]. A 3–5 square micron region in the middle of cilia lying horizontal in a single confocal z plane was bleached (Figure 4A). Fluorescence within the bleached region was normalized to account for both prebleach intensity and photobleaching of the sample during recovery. Single exponential fit of the averaged data revealed that nearly 75% of the fluorescent signal recovers with a time constant of approximately 600 s. (Figure 4B). The fact that 25% of the channel is immobile or of limited mobility would have been predicted based on its role as

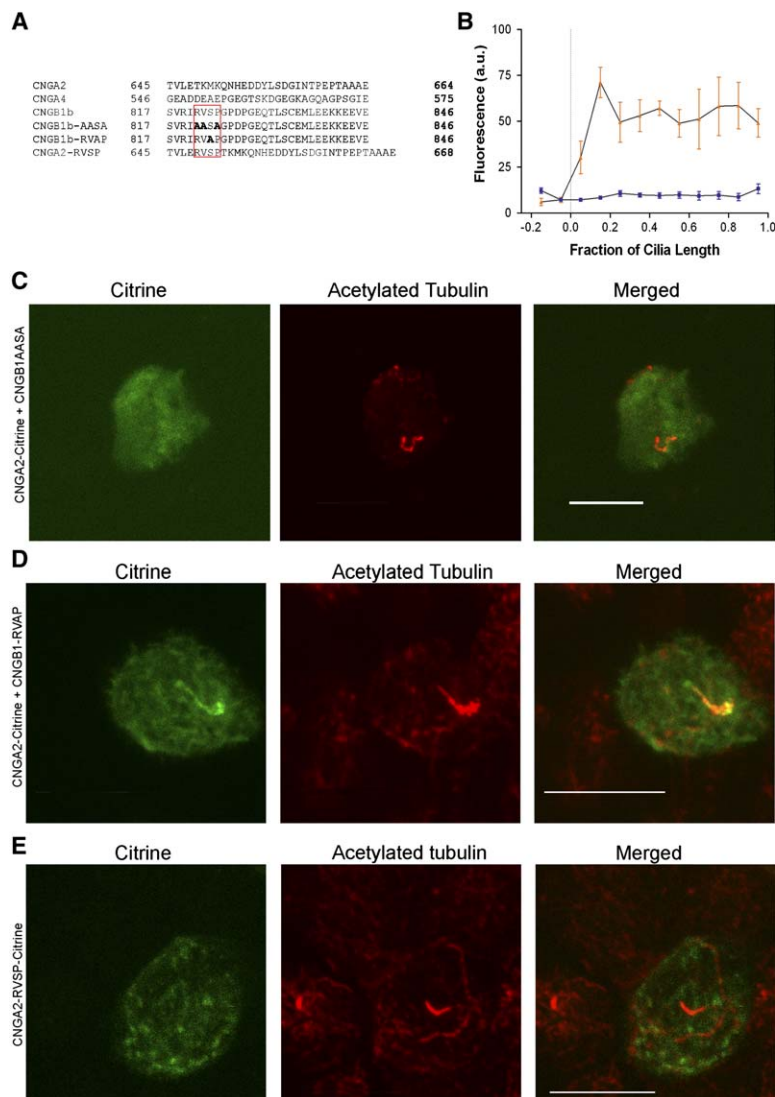


Figure 2. A Carboxyl-Terminal Motif in CNGB1b Is Necessary but Not Sufficient for Ciliary Trafficking of CNG Channels

(A) Sequence alignment of final 30 carboxyl-terminal amino acids of wild-type CNGA2, CNGA4, CNGB1b, and mutant constructs. Alignment of the RVxP motif in CNG channel constructs is outlined in the red box. Amino acid substitutions and insertions are shown in bold.

(B) Plot of normalized fractional cilia length versus average fluorescence intensity in arbitrary units (a.u.) for both channel signal (blue) and acetylated tubulin (orange) in cells expressing CNGA2-citrine and CNGB1b-AASA-3xFlag (n = 3). Dotted line marks the beginning of cilia as determined by concentrated acetylated tubulin signal. Values are mean \pm SEM.

(C) Representative image of MDCK cell transfected with CNGA2-citrine (green, left) and + CNGB1b-AASA-3xFlag mutant and immunostained with antiacetylated tubulin (red, center) shown with merged image (right). Scale bar represents 10 μ m.

(D) Representative image of MDCK cell transfected with CNGA2-citrine (green) and CNGB1b-RVAP-3xFlag. Acetylated tubulin shown in (red). Merged image shown on right with yellow indicating colocalization. Scale bar represents 10 μ m.

(E) Representative image of MDCK cell transfected with CNGA2-RVSP-citrine. Acetylated tubulin shown in (red). Scale bar represents 10 μ m.

a transmembrane signaling protein [22]. Recovery of fluorescent channel signal in the cell body was nearly four times more rapid (Figure S8), illustrating the differences in ciliary and cellular trafficking. Fluorescence recovery in the cilia occurred from both sides of the bleached region (Figure S8). As a chemosensory-signaling protein, the vast majority of ciliary CNG channel is likely localized within the plasma membrane. Technical limitations hinder the ability to resolve the combination of lateral diffusion within the plasma membrane and recovery because of IFT. The recovery time course in our experiments, therefore, most likely reflects membrane diffusion of a large population of channels that masks the minority of CNG protein undergoing IFT. This is supported by the fact that CNG channel recovery in cilia occurred slower than predicted for IFT (rates of 1–2 μ m/s). Of note, a similar time constant of recovery on the order of hundreds of seconds was recently reported for the lipid raft-associated Kv2.1 channel [23]. As CNGA2 targets to lipid raft microdomains [24], perhaps raft association confines the channel to a restricted diffusional microdomain.

Discussion

Our studies demonstrate that heteromeric assembly with CNGB1b is needed for localization of olfactory CNG channels to cilia in MDCK cells. An RVxP motif conserved across species (including human) is necessary, but not sufficient, for ciliary targeting; however, its position within the CNGB1b sequence can vary. These results demonstrate a mechanistic role of CNGB1b subunits in proper ciliary targeting of olfactory CNG channels and suggest a delegation of functional responsibilities among subunits.

Our results constitute the first demonstration of a role for KIF17 in mammalian ciliary transport. This kinesin-2 motor is not brain specific [12] but rather is present in both MDCK cell cilia and OSNs. In vertebrate sensory cilia, the Kif3a complex and KIF17 likely have partially redundant yet functionally distinct roles in IFT because the KIF3aDN resulted in a complete loss of cilia, whereas the KIF17DN did not change average cilia length. This work provides strong support for the idea that OSM-3/KIF17 is an “accessory” IFT motor whose cilia-specific

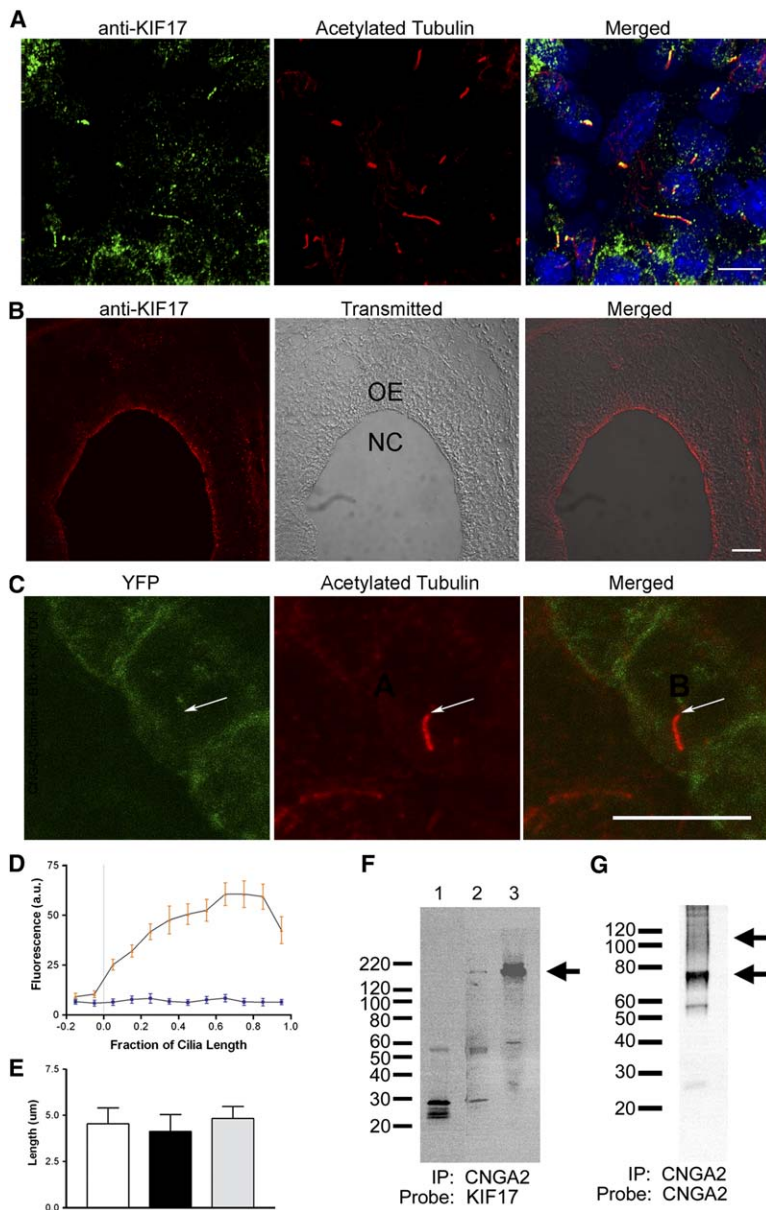


Figure 3. KIF17 Is Endogenously Expressed in Both MDCK Cells and OSNs and Mediates Ciliary Enrichment of the CNG Channel

(A) Untransfected MDCK cells stained with rabbit polyclonal anti-KIF17 (green) and mouse monoclonal anti-acetylated tubulin (red). Overlay shows merged images together with nuclear staining by using DAPI (blue); yellow indicates colocalization. Bar represents 10 μ m.

(B) Mouse olfactory epithelium stained with rabbit polyclonal anti-KIF17 antibodies (red). Olfactory epithelium (OE), nasal cavity (NC). Bar represents 50 μ m.

(C) Representative image of MDCK cell transfected with CNGA2-citrine, CNGB1b-3 \times Flag, and myc-KIF17DN (801–1028). Arrowhead marks base of cilium. Signal shown from CNGA2-citrine fluorescence (left, green), acetylated tubulin immunostaining (center, red), and merge (right). Bar represents 10 μ m.

(D) Plot of normalized fractional cilia length versus average fluorescence intensity in arbitrary units (a.u.) for both channel signal (blue) and acetylated tubulin (orange) from MDCK cells expressing CNGA2-citrine, CNGB1b-3 \times Flag, and myc-KIF17DN (n = 11). Dotted line marks the beginning of cilia as determined by concentrated acetylated tubulin signal. Values are mean \pm SEM.

(E) Average length of analyzed cilia from MDCK cells transfected with CNGA2-citrine, B1b-3 \times Flag, and either no KIF17 (white, n = 14), KIF17DN (black, n = 10), or KIF17 full-length (gray, n = 5) constructs. KIF17DN had no statistically significant effect on cilia length (p = 0.7564, one-way ANOVA). Values are mean \pm SEM.

(F) KIF17 immunoprecipitates with CNGA2 in native rat olfactory epithelium. Lane 1 represents immunoprecipitation with nonspecific IgG as a negative control. Lane 2 shows immunoprecipitation with anti-CNGA2 antibodies (1:200), and lane 3 is the starting material from rat olfactory epithelium. Blots were probed with anti-KIF17 (1:1000). Arrow indicates band for Kif17 with an approximate molecular weight of 170 kDa.

(G) Lane 2F was stripped and reprobed with anti-CNGA2 antibodies (1:200). Arrows indicate bands for CNGA2 with the lower, nonglycosylated form running at approximately 75 kDa and the upper glycosylated form running as a smear between 90–150 kDa.

functions can cooperate with, yet functionally complement, the “canonical” Kif3a IFT motor [9–11]. Future experiments are required to determine whether KIF17 is important for the transport of other ciliary proteins or if this motor functions primarily on singlet microtubules at the distal segments. Interestingly, a recent report shows that a majority of olfactory CNG channels are localized to the distal segments of frog olfactory cilia [25]. The possibility remains that the Kif3a complex also contributes to ciliary targeting of CNG channels because expression of the KIF3aDN led to a complete loss of cilia. In addition, our work also does not exclude the role of additional uncharacterized motors such as a mammalian homolog to the recently described KLP-6 in *C. elegans* [26].

List of Abbreviations

CNG, cyclic nucleotide-gated channel; MDCK, Madin Darby canine kidney cells; OSN, olfactory sensory neuron; BBS: Bardet-Biedl syndrome; IFT, intraflagellar transport; FRAP, fluorescence recovery after photobleaching; YFP, yellow-fluorescent protein; AC-III, adenylyl cyclase type III.

Experimental Procedures

Detailed Experimental Procedures can be found in [Supplemental Data](#).

Supplemental Data

Supplemental Data include 8 figures and Supplemental Experimental Procedures and can be found with this article online at <http://www.current-biology.com/cgi/content/full/16/12/1211/DC1/>.

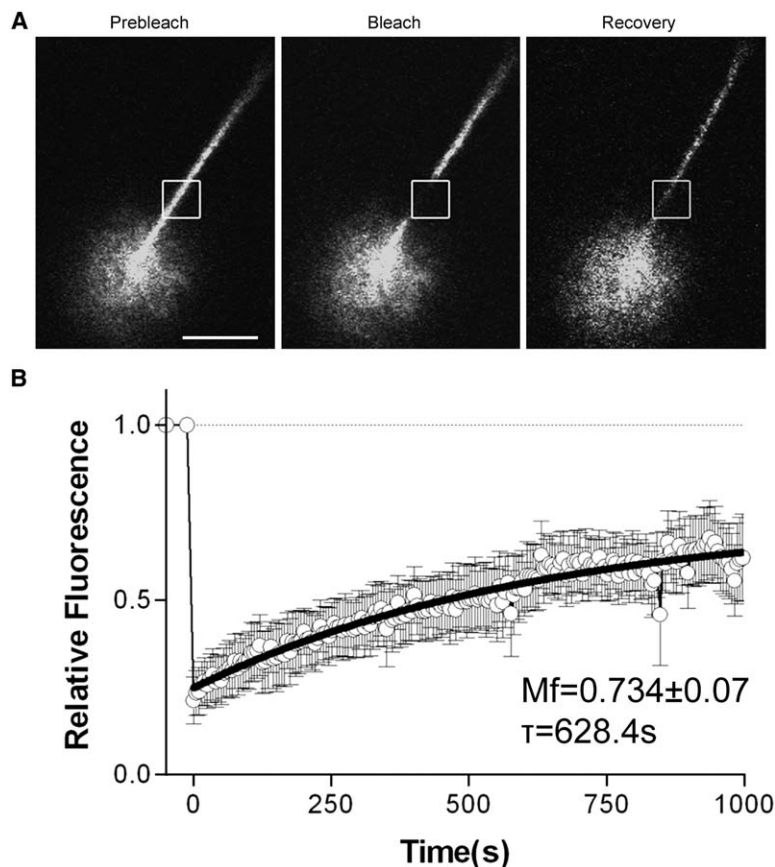


Figure 4. A Significant Fraction of CNG Channels Is Mobile in the Primary Cilia of MDCK Cells

(A) Selected images from a confocal FRAP experiment at 25°C in living MDCK cells transfected with CNGA2-citrine and CNGB1b-3×Flag showing fluorescence signal from CNGA2-citrine in cilia prebleach, immediately postbleach ($t = 0$ s), and after recovery ($t = 600$ s). Box represents area of photobleach (dimensions of box). Bar represents 5 μm .

(B) Average recovery after photobleach for CNGA2-citrine signal from the cilia of MDCK cells. Data shown are mean \pm SE, $n = 5$ cells. The solid line through the data is a single-exponential fit to the average data. Fit parameters: mobile fraction = 0.734 ± 0.07 , $\tau = 628.4$ s, $R^2 = 0.952$.

Acknowledgments

We would like to thank Dr. U. Benjamin Kaupp at the Institut für Biologische Informationsverarbeitung, Jülich, Germany for generously providing the antibody to CNGA2. This publication was supported by grant number GM07767 from National Institute of General Medical Sciences (P.M.J.), grant numbers EY12837 (R.L.B.) and DK069605 (B.M.) from the National Institutes of Health, and grant number 92a2f from the Polycystic Kidney Disease Foundation (T.W.H.).

Received: February 3, 2006

Revised: April 14, 2006

Accepted: April 19, 2006

Published: June 19, 2006

References

1. Firestein, S., and Werblin, F. (1989). Odor-induced membrane currents in vertebrate-olfactory receptor neurons. *Science* 244, 79–82.
2. Nakamura, T., and Gold, G.H. (1987). A cyclic nucleotide-gated conductance in olfactory receptor cilia. *Nature* 325, 442–444.
3. Ronnett, G.V., and Moon, C. (2002). G proteins and olfactory signal transduction. *Annu. Rev. Physiol.* 64, 189–222.
4. Bonigk, W., Bradley, J., Muller, F., Sesti, F., Boekhoff, I., Ronnett, G.V., Kaupp, U.B., and Frings, S. (1999). The native rat olfactory cyclic nucleotide-gated channel is composed of three distinct subunits. *J. Neurosci.* 19, 5332–5347.
5. Trudeau, M.C., and Zagotta, W.N. (2002). An intersubunit interaction regulates trafficking of rod cyclic nucleotide-gated channels and is disrupted in an inherited form of blindness. *Neuron* 34, 197–207.
6. Huttli, S., Michalakakis, S., Seeliger, M., Luo, D.G., Acar, N., Geiger, H., Hudl, K., Mader, R., Haverkamp, S., Moser, M., et al. (2005). Impaired channel targeting and retinal degeneration in mice lacking the cyclic nucleotide-gated channel subunit CNGB1. *J. Neurosci.* 25, 130–138.
7. Rosenbaum, J.L., and Witman, G.B. (2002). Intraflagellar transport. *Nat. Rev. Mol. Cell Biol.* 3, 813–825.
8. Scholey, J.M. (2003). Intraflagellar transport. *Annu. Rev. Cell Dev. Biol.* 19, 423–443.
9. Evans, J.E., Snow, J.J., Gunnarson, A.L., Ou, G., Stahlberg, H., McDonald, K.L., and Scholey, J.M. (2006). Functional modulation of IFT kinesins extends the sensory repertoire of ciliated neurons in *Caenorhabditis elegans*. *J. Cell Biol.* 172, 663–669.
10. Ou, G., Blacque, O.E., Snow, J.J., Leroux, M.R., and Scholey, J.M. (2005). Functional coordination of intraflagellar transport motors. *Nature* 436, 583–587.
11. Snow, J.J., Ou, G., Gunnarson, A.L., Walker, M.R., Zhou, H.M., Brust-Mascher, I., and Scholey, J.M. (2004). Two anterograde intraflagellar transport motors cooperate to build sensory cilia on *C. elegans* neurons. *Nat. Cell Biol.* 6, 1109–1113.
12. Setou, M., Nakagawa, T., Seog, D.H., and Hirokawa, N. (2000). Kinesin superfamily motor protein KIF17 and mLin-10 in NMDA receptor-containing vesicle transport. *Science* 288, 1796–1802.
13. Zheng, J., and Zagotta, W.N. (2004). Stoichiometry and assembly of olfactory cyclic nucleotide-gated channels. *Neuron* 42, 411–421.
14. Geng, L., Okuhara, D., Yu, Z., Tian, X., Cai, Y., Shibazaki, S., and Somlo, S. (2006). Polycystin-2 traffics to cilia independently of polycystin-1 by using an N-terminal RVXP motif. *J. Cell Sci.* 119, 1383–1395.
15. Snapp, E.L., and Landfear, S.M. (1999). Characterization of a targeting motif for a flagellar membrane protein in *Leishmania enriettii*. *J. Biol. Chem.* 274, 29543–29548.
16. Nishimura, T., Kato, K., Yamaguchi, T., Fukata, Y., Ohno, S., and Kaibuchi, K. (2004). Role of the PAR-3-KIF3 complex in the establishment of neuronal polarity. *Nat. Cell Biol.* 6, 328–334.
17. Lin, F., Hiesberger, T., Cordes, K., Sinclair, A.M., Goldstein, L.S., Somlo, S., and Igarashi, P. (2003). Kidney-specific inactivation of the KIF3A subunit of kinesin-II inhibits renal ciliogenesis

- and produces polycystic kidney disease. *Proc. Natl. Acad. Sci. USA* **100**, 5286–5291.
18. Marszalek, J.R., Liu, X., Roberts, E.A., Chui, D., Marth, J.D., Williams, D.S., and Goldstein, L.S. (2000). Genetic evidence for selective transport of opsin and arrestin by kinesin-II in mammalian photoreceptors. *Cell* **102**, 175–187.
 19. Noda, Y., Okada, Y., Saito, N., Setou, M., Xu, Y., Zhang, Z., and Hirokawa, N. (2001). KIFC3, a microtubule minus end-directed motor for the apical transport of annexin XIIIb-associated Triton-insoluble membranes. *J. Cell Biol.* **155**, 77–88.
 20. Bakalyar, H.A., and Reed, R.R. (1990). Identification of a specialized adenylyl cyclase that may mediate odorant detection. *Science* **250**, 1403–1406.
 21. Griesbeck, O., Baird, G.S., Campbell, R.E., Zacharias, D.A., and Tsien, R.Y. (2001). Reducing the environmental sensitivity of yellow fluorescent protein. Mechanism and applications. *J. Biol. Chem.* **276**, 29188–29194.
 22. Saxton, M.J., and Jacobson, K. (1997). Single-particle tracking: applications to membrane dynamics. *Annu. Rev. Biophys. Biomol. Struct.* **26**, 373–399.
 23. O'Connell, K.M., and Tamkun, M.M. (2005). Targeting of voltage-gated potassium channel isoforms to distinct cell surface microdomains. *J. Cell Sci.* **118**, 2155–2166.
 24. Brady, J.D., Rich, T.C., Le, X., Stafford, K., Fowler, C.J., Lynch, L., Karpen, J.W., Brown, R.L., and Martens, J.R. (2004). Functional role of lipid raft microdomains in cyclic nucleotide-gated channel activation. *Mol. Pharmacol.* **65**, 503–511.
 25. Flannery, R.J., French, D.A., and Kleene, S.J. (2006). Clustering of cyclic-nucleotide-gated channels in olfactory cilia. *Biophys. J.*, in press. Published online April 7, 2006. 10.1529/biophysj.105.079046.
 26. Peden, E.M., and Barr, M.M. (2005). The KLP-6 kinesin is required for male mating behaviors and polycystin localization in *Caenorhabditis elegans*. *Curr. Biol.* **15**, 394–404.